Electronic Supplementary Material (ESI) for Inorganic Chemistry Frontiers.

Monocrystalline Orthorhombic $Na_{0.44}Mn_{0.9}Li_{0.1}O_2$ Cathode with Outstanding Stability and Negligible Structural Strain for Sodium-Ion Batteries

Tao Chen [a1], Xiaowen Fan [a1], Yi Zhuo [a], Baixue Ouyang [a], Xinxin Chen [a], Kaiyu Liu*[a]

Abstract: The application of sodium ion batteries (SIBs) in future large-scale energy storage equipment is facing great challenges due to its unstable cathode materials. Herein, monocrystalline orthorhombic $Na_{0.44}Mn_{0.9}Li_{0.1}O_2$ with high crystallinity has been designed and synthesized via a simple sol–gel method. The wide tunnel structure of $Na_{0.44}Mn_{0.9}Li_{0.1}O_2$ can not only adapt to structural strain in the electrochemical process, but also provide the rapid migration path for Na^+. Furthermore, the introduction of Li promotes the transformation from trivalent manganese to tetravalent manganese so that the structural distortion caused by Jahn-Teller effect is effectively alleviated. High Na+ mobility and low Na+ diffusion resistance are another guarantee of its excellent rate performance. As a consequence, $Na_{0.44}Mn_{0.9}Li_{0.1}O_2$ electrode delivers an initial discharge capacity of 111.71 mAh g^{-1} at 1 C with extreme retention of 80% after 900 cycles. So far, to the best of our knowledge, the as-systhesized $Na_{0.44}Mn_{0.9}Li_{0.1}O_2$ shows the most exellent stability at 1 C. Such a material with superior stability and high rate performance is suggested to be one of the promising cathodes for SIBs.

Table of Contents

Figure S1. XRD patterns of NM. 2
Figure S2.Cycling performance of NML at 0.2C. 2
Figure S3. Average voltage of NML and NM. 3
Figure S4. (a) Cycling performance of NML0.2 at 1C; (b) Charge-discharge profiles of different cycles at 1C. 3
Figure S5. Rate capabilities of NML and NM. 3
Figure S6. CV profiles of NML and NM in the thired cycle within the voltage range of 2.0-4.0V. 4
Figure S7. E-τ plot of single titration of NML during the charging process. 4
Figure S8.Linear fitting diagram of E-$\tau^{1/2}$ during charging process. 5
Figure S9. E-τ plot of single titration of NML during the discharging process. 5
Figure S10. Linear fitting diagram of E-$\tau^{1/2}$ during charging process. 6
Table S1. ICP results of $Na_{0.44}Mn_{0.9}Li_{0.1}O_2$ and $Na_{0.44}MnO_2$ sample. 6
Table S2. Crystallographic parameters of $Na_{0.44}Mn_{0.9}Li_{0.1}O_2$ refined by the Rietveld method. 6
Table S3. Redox peak and mechanism in CV curve of NML 7
Table S4. Summary of Na^+ diffusion coefficients for sodium ion batteries in recent years. 7
Table S5 Fitting parameters for the equivalent circuit model shown in Fig 6c 8

Results and Discussion

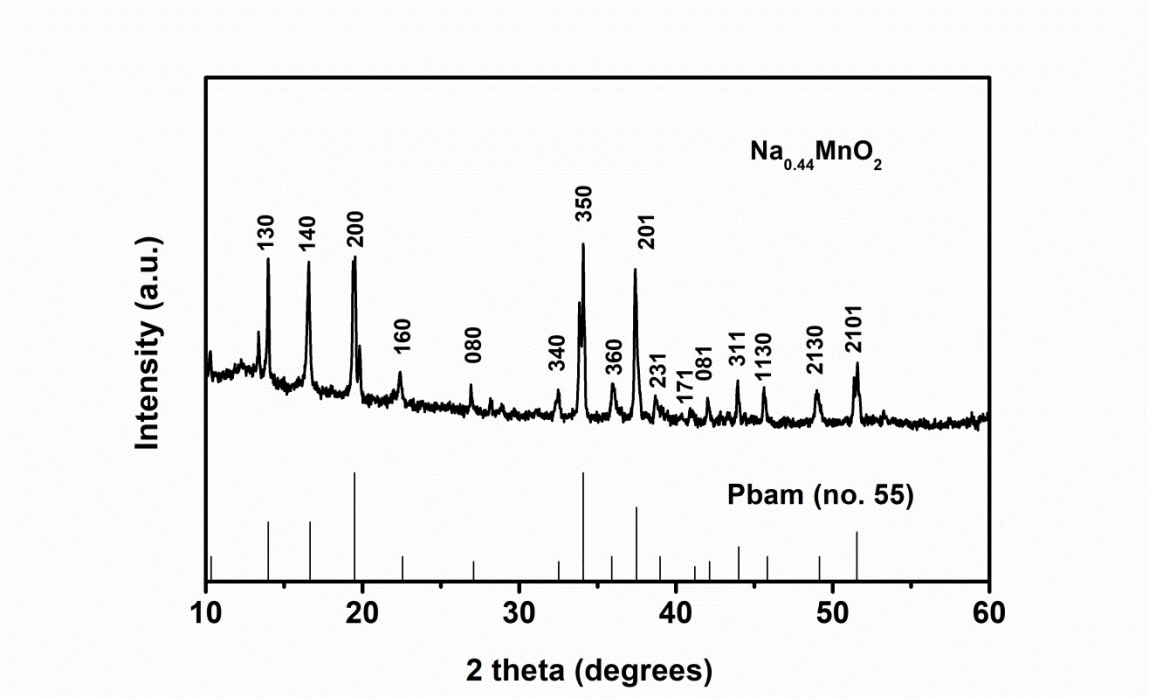

Figure S1. XRD patterns of NM.

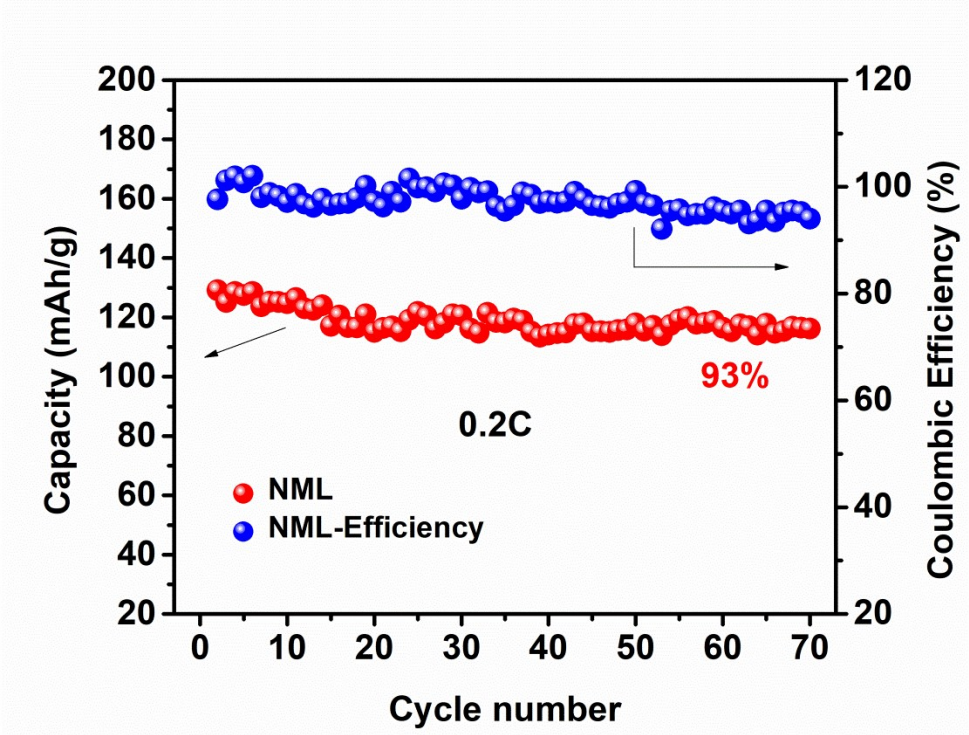

Figure S2. Cycling performance of NML at 0.2C.

Figure S3. Average voltage of NML and NM.

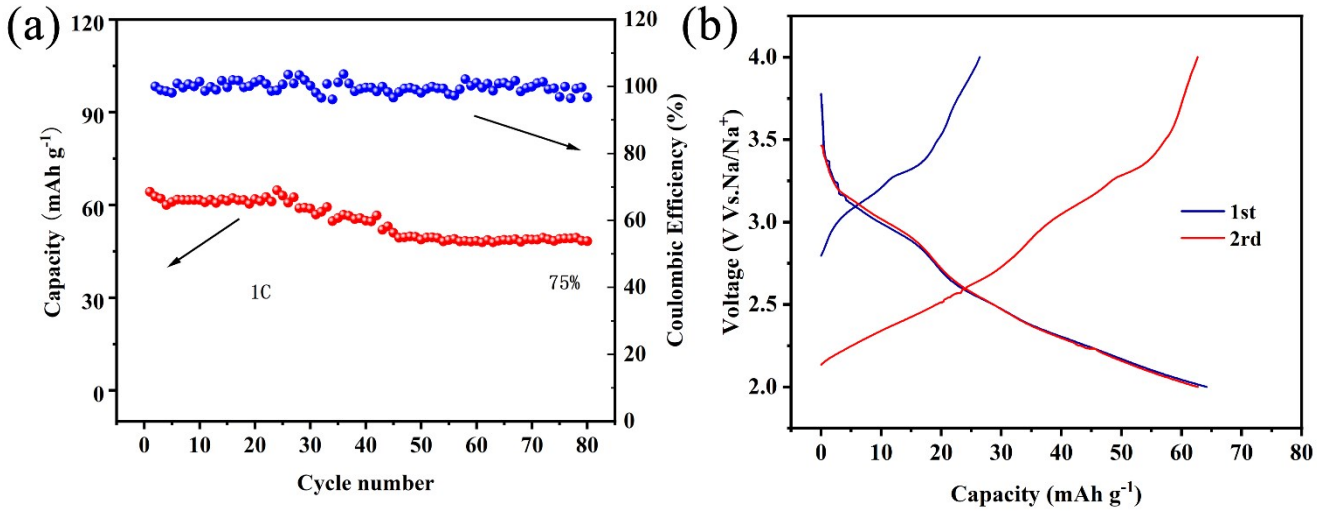

Figure S4. (a) Cycling performance of NML0.2 at 1C; (b) Charge-discharge profiles of different cycles at 1C.

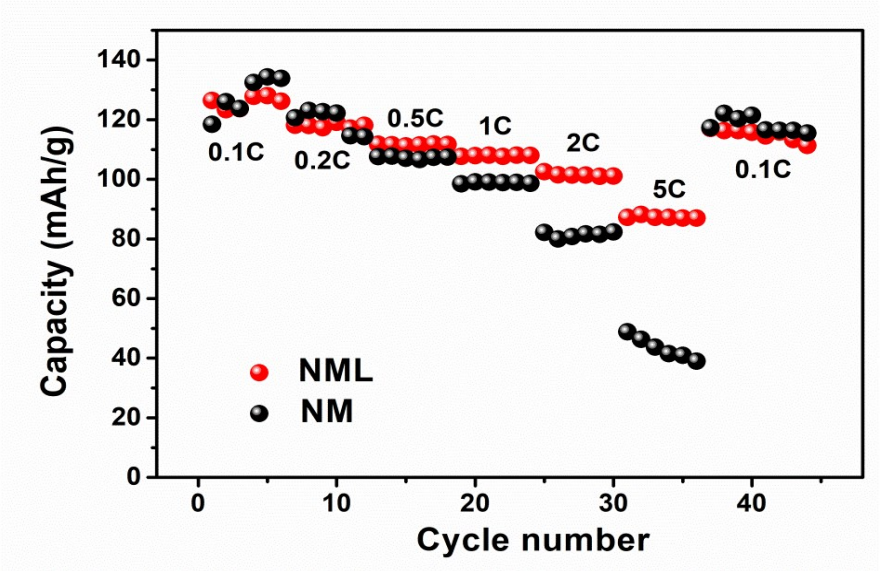

Figure S5. Rate capabilities of NML and NM.

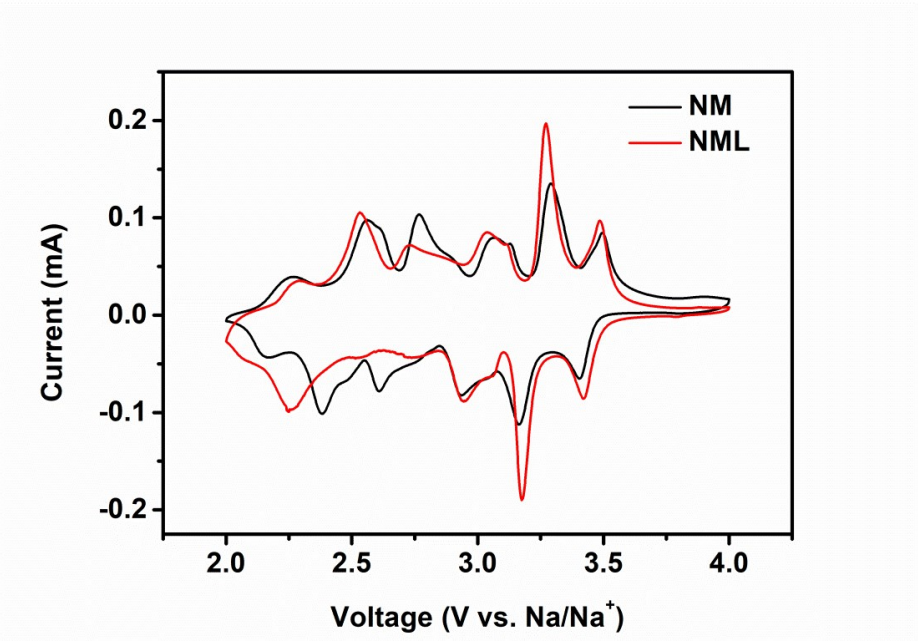

Figure S6. CV profiles of NML and NM in the thired cycle within the voltage range of 2.0-4.0V.

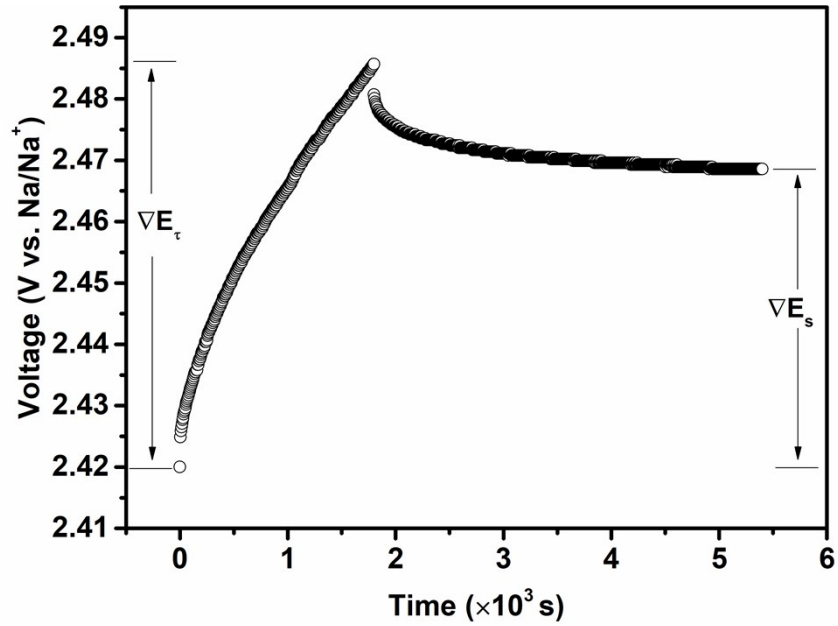

Figure S7. E-τ plot of single titration of NML during the charging process.

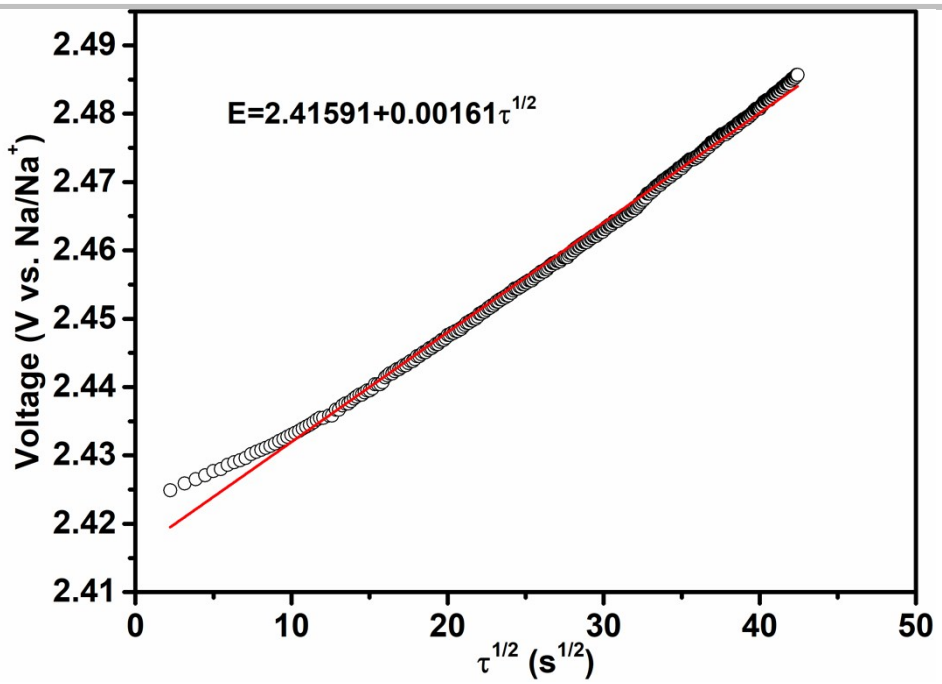

Figure S8.Linear fitting diagram of E-$\tau^{1/2}$ during charging process.

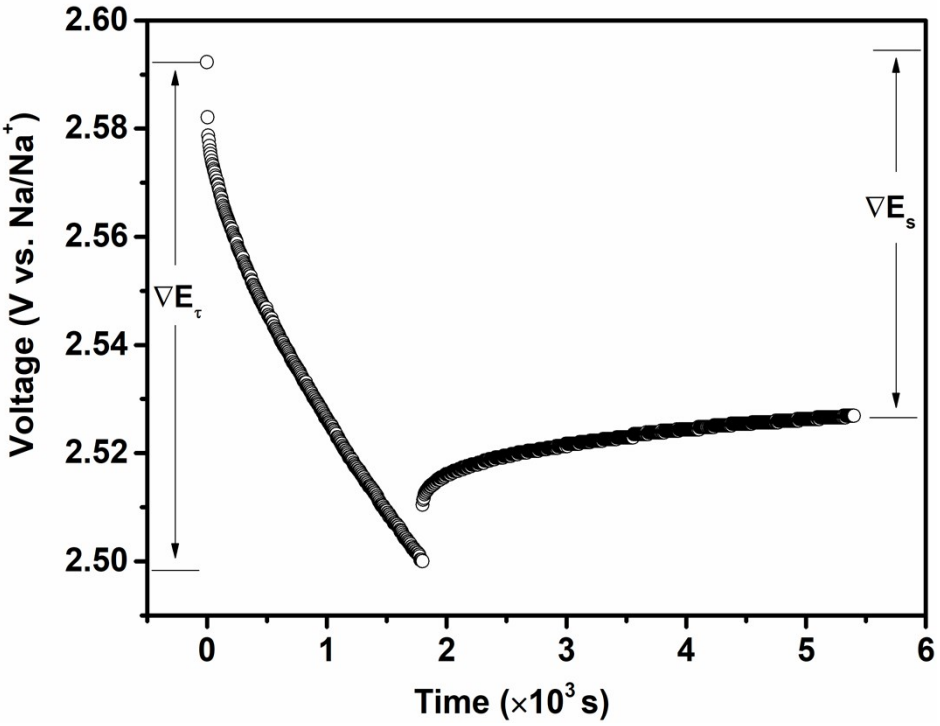

Figure S9. E-τ plot of single titration of NML during the discharging process.

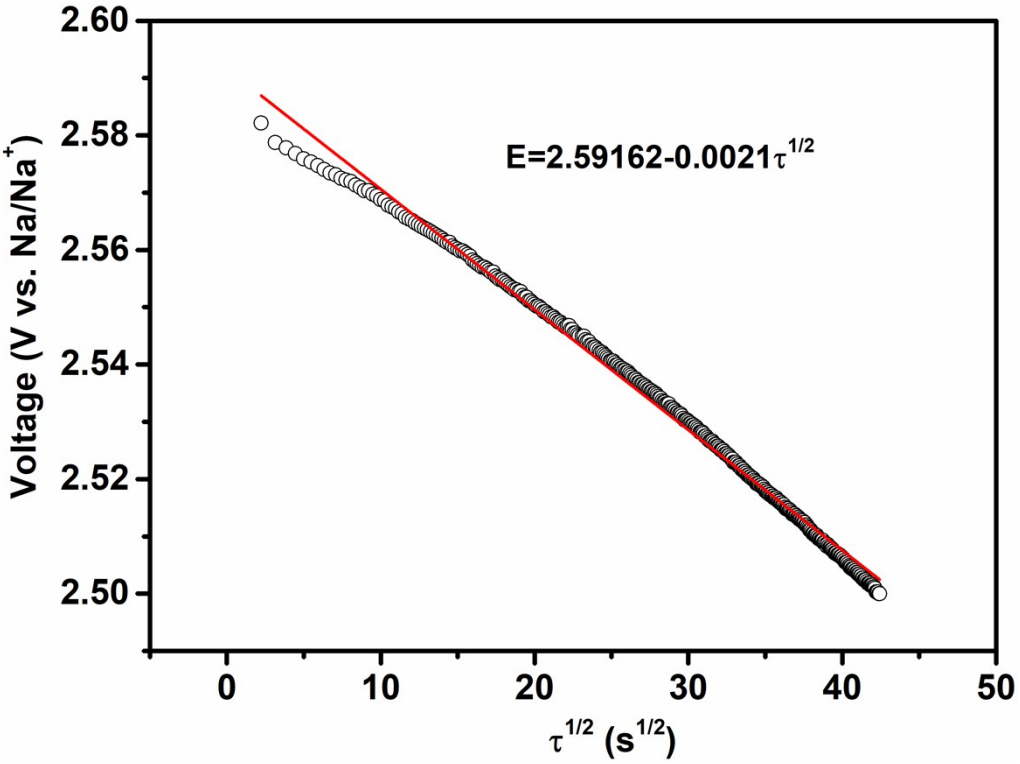

Figure S10. Linear fitting diagram of E-$\tau^{1/2}$ during charging process.

Table S1. ICP results of $Na_{0.44}Mn_{0.9}Li_{0.1}O_2$ and $Na_{0.44}MnO_2$ sample.

samples	Measured atomic ratio		
	Na	Mn	Li
$Na_{0.44}Mn_{0.9}Li_{0.1}O_2$	0.4407	0.9032	0.0968
$Na_{0.44}MnO_2$	0.4378	1.0202	0

Table S2. Crystallographic parameters of $Na_{0.44}Mn_{0.9}Li_{0.1}O_2$ refined by the Rietveld method.

	$Na_{0.44}Mn_{0.9}Li_{0.1}O_2$
Space group Pbam(No.55)	
Rwp	2.41%
Rp	1.81%
χ^2	1.742
a(Å)	9.08265(6)
b(Å)	26.35667(4)
c(Å)	2.82499(2)
V(Å3)	676.27(1)

Table S3. Redox peak and mechanism in CV curve of NML

Anodic peak(V)	cathodic peak(V)	Difference(V)	Mechanism
2.28	2.09	0.19	1/4 Na3
2.53	2.26	0.27	1/4 Na2
2.73	2.55	0.18	1/4 Na3 + 1/4 Na1
3.04	2.95	0.09	1/4 Na2
3.27	3.17	0.10	1/4 Na2 + 1/4 Na1
3.48	3.42	0.06	1/4 Na2

Table S4. Summary of Na^+ diffusion coefficients for sodium ion batteries in recent years.

Cathode materials	D_{Na} (cm^{-2} s^{-1})	Method	Ref.
$Na_{0.44}Mn_{0.89}Ti_{0.11}O_2$	$3.6 \times 10^{-15} - 8.6 \times 10^{-14}$	GITT	[1]
$Na_{0.44}MnO_2$ NWs	1.17×10^{-13}	GITT	[2]
$Na_{0.44}MnO_2$ NF	$2.98 \times 10^{-16} - 5.60 \times 10^{-15}$	GITT	[3]
$Na_{0.44}MnO_2$ NR	$0.81 \times 10^{-19} - 1.46 \times 10^{-18}$	GITT	[3]
$Na_{0.67}Mn_{0.55}Ni_{0.25}Li_{0.2}O_2$	9.81×10^{-14}	PITT	[4]
$Na_{2/3}Fe_{2/9}Ni_{2/9}Mn_{5/9}O_2$	$10^{-12} - 10^{-11}$	GITT	[5]
$Na_{2/3}Fe_{1/2}Mn_{1/2}O_2$	1.83×10^{-13}	GITT	[6]
$Na_{2/3}Ni_{1/3}Mn_{5/9}Al_{1/9}O_2$	2.49×10^{-12}	GITT	[7]
$Na_{0.62}Ti_{0.37}Cr_{0.63}O_2$	$2 \times 10^{-13} - 1 \times 10^{-12}$	GITT	[8]
$Na_{0.44}Mn_{0.9}Li_{0.1}O_2$	$0.25 \times 10^{-10} - 2.27 \times 10^{-10}$	GITT	This work

Table S5 Fitting parameters for the equivalent circuit model shown in Fig 6c

	R_Ω	R_f	R_{ct}	Total(R_Ω+R_f+R_{ct})
5th cycles	11.93	19.97	9.205	53.035
50th cycles	10.19	15.07	7.993	33.253

[1] W.-J. Shi, D. Zhang, X.-M. Meng, C.-X. Bao, S.-D. Xu, L. Chen, X.-M. Wang, S.-B. Liu, Y.-C. Wu, Low-Strain Reticular Sodium Manganese Oxide as an Ultrastable Cathode for Sodium-Ion Batteries, *Acs Applied Materials & Interfaces*, 2020, **12**, 14174-14184.

[2] Y. Liu, X. Liu, F. Bu, X. Zhao, L. Wang, Q. Shen, J. Zhang, N. Zhang, L. Jiao, L.-Z. Fan, Boosting fast and durable sodium-ion storage by tailoring well-shaped $Na_{0.44}MnO_2$ nanowires cathode, *Electrochimica Acta*, 2019, **313**, 122-130.

[3] B. Fu, X. Zhou, Y.P. Wang, High-rate performance electrospun $Na_{0.44}MnO_2$ nanofibers as cathode material for sodium-ion batteries, *Journal Of Power Sources*, 2016, **310**, 102-108.

[4] Z.-Y. Li, J. Zhang, R. Gao, H. Zhang, L. Zheng, Z. Hu, X. Liu, Li-Substituted Co-Free Layered P2/O3 Biphasic $Na_{0.67}Mn_{0.55}Ni_{0.25}Ti_{0.2-x}Li_xO_2$ as High-Rate-Capability Cathode Materials for Sodium Ion Batteries, *Journal Of Physical Chemistry C*, 2016, **120**, 9007-9016.

[5] Y. Zhang, M. Wu, J. Ma, G. Wei, Y. Ling, R. Zhang, Y. Huang, Revisiting the $Na_{2/3}Ni_{1/3}Mn_{2/3}O_2$ Cathode: Oxygen Redox Chemistry and Oxygen Release Suppression, *Acs Central Science*, 2020, **6**, 232-240.

[6] M. Li, D.L. Wood, Y. Bai, R. Essehli, M.R. Amin, C.J. Jafta, N. Muralidharan, J. Li, I. Belharouak, Eutectic Synthesis of P2-Type $NaxFe_{1/2}Mn_{1/2}O_2$ Cathode with Improved Cell Design for Sodium-Ion Batteries, *ACS applied materials & interfaces*, 2020, 12, 23951–23958.

[7] X.-H. Zhang, W.-L. Pang, F. Wan, J.-Z. Guo, H.-Y. Lu, J.-Y. Li, Y.-M. Xing, J.-P. Zhang, X.-L. Wu, P2-$Na_{2/3}Ni_{1/3}Mn_{5/9}Al_{1/9}O_2$ Microparticles as Superior Cathode Material for Sodium-Ion Batteries: Enhanced Properties and Mechanisam via Graphene Connection, *Acs Applied Materials & Interfaces*, 2016, **8**, 20650-20659.

[8] S. Guo, J. Yi, Y. Sun, H. Zhou, Recent advances in titanium-based electrode materials for stationary sodium-ion batteries, *Energy & Environmental Science*, 2016, **9**, 2978-3006.